

Published in final edited form as:

J Neurosci. 2012 February 15; 32(7): 2252–2262. doi:10.1523/JNEUROSCI.5493-11.2012.

Tamalin is a critical mediator of electroconvulsive shock-induced adult neuroplasticity

Sudhirkumar U. Yanpallewar, Colleen A. Barrick, Mary Ellen Palko, Gianluca Fulgenzi, and Lino Tessarollo*

Neural Development Section, Mouse Cancer Genetics Program, Center for Cancer Research, NCI, Frederick, MD, 21702, USA

Abstract

The molecular mechanisms underlying the effects of electroconvulsive shock therapy (ECS), a fast acting and very effective anti-depressant therapy, are poorly understood. Changes related to neuroplasticity, including enhanced adult hippocampal neurogenesis and neuronal arborization, are believed to play an important role in mediating the effects of ECS. Here we show a dynamic up-regulation of the scaffold protein tamalin, selectively in the hippocampus of animals subjected to ECS. Interestingly, this gene up-regulation is functionally significant since tamalin deletion in mice abrogated ECS-induced neurogenesis in the adult mouse hippocampus. Furthermore, loss of tamalin blunts mossy fiber sprouting and dendritic arborization caused by ECS. These data suggest an essential role for tamalin in ECS-induced adult neuroplasticity and provide new insight into the pathways that are involved in mediating ECS effects.

Introduction

Electroconvulsive shock (ECS) is an effective and fast acting therapy for patients with major depression. Unlike drug therapy, which requires several weeks to exert its effect, ECS can provide both immediate relief from depression, possibly by affecting immediate neurochemical alterations, and long-term effects by affecting neuroplasticity (Malberg et al., 2000). The changes in neuroplasticity include increased adult neurogenesis and neuronal sprouting in the hippocampus. ECS animal studies have shown that a wide variety of molecules, including neurotrophins, neurotransmitters, neuropeptides and their receptors, undergo significant changes in expression (Altar et al., 2004). Other proteins such as those with scaffolding activity also show expression changes following ECS and are of particular interest because they are capable of affecting multiple pathways inducing both short-term as well as long-term changes. For example, homer-1a is significantly up-regulated by ECS and its injection into rats regulates neuronal excitability (Sakagami et al., 2005). Moreover, homer1a affects both signal transduction as well as cytoskeletal rearrangements (Fagni et al., 2002). Despite the identification of genes whose expression changes during ECS, it is still unclear which molecules and pathways are essential for mediating its effects (Altar et al., 2004; Kato, 2009).

Tamalin is a scaffold protein that interacts with group 1 metabotropic receptors (mGluR1 and 5), a truncated isoform of the neurotrophin-3 receptor TrkC and multiple postsynaptic and protein-trafficking scaffold proteins (Esteban et al., 2006; Hirose et al., 2004; Kitano et al., 2003). Tamalin mRNA expression is highest in brain areas, such as the hippocampus that undergo significant structural plasticity. While it is not required for normal brain development, tamalin deficiency in the mouse reduces morphine and cocaine sensitivity,

* Author for correspondence: tessarol@mail.nih.gov.

probably by affecting the adaptive neural plasticity involved in reinforcement and addiction in drug abuse (Ogawa et al., 2007).

These results prompted us to investigate whether tamalin could influence adaptive neural plasticity occurring in other paradigms. In this study, we found a robust increase in tamalin expression in response to kainate and ECS. Moreover, in contrast to the increased hippocampal neurogenesis and neuronal sprouting observed in wild type (WT) mice subjected to ECS, mice lacking tamalin had a blunted response. Thus, tamalin is dispensable for development but is required to mediate ECS-induced adult hippocampal neuroplasticity.

Materials and Methods

Electroconvulsive Shock Treatment

ECS was administered via bilateral ear clip electrodes using an Ugo Basile ECS unit (Model 57800) (Vaidya et al., 1999). Animals received sham treatment or ECS (Current-18mA, Shock Duration- 0.5 sec, Frequency- 100 pulses/sec and Pulse Width- 0.5 ms) for 1, 5 or 10 consecutive days and were euthanized at specific time-points depending on the analysis.

To evaluate the changes in tamalin mRNA expression, WT animals were subjected to sham or a single ECS treatment, and sacrificed at 1, 3, 6, 12 and 24h. For chronic treatment, a set of animals was subjected to ECS or sham treatment daily, for 5 consecutive days and sacrificed 24h after the last treatment. Animals were perfused with 4% paraformaldehyde (PFA), after which their brains were removed and processed for in situ hybridization.

Kainate Treatment

Adult mice were injected with kainate (10mg/kg, intraperitoneal, Sigma) or vehicle as previously described (Jiang et al., 2008). After 3h, they were sacrificed and perfused with 4% PFA. Coronal brain sections were then taken for in situ hybridization or immunohistochemistry analysis.

In situ hybridization

Digoxygenin (Dig) in situ hybridization protocols using the sense or anti-sense full-length tamalin (Esteban et al., 2006) and homer1a (a gift from Dr. Mehdi Tafti, University of Lausanne, Switzerland) riboprobes were performed as follows. Dig-labelled RNA probes were synthesized by using the Promega Riboprobe system. Serial cryostat coronal sections (50 μ m) were proteinase K-treated (5 μ g/ml) in PBS and post-fixed in 4% PFA. Sections were then incubated in hybridization buffer (50% formamide, 5X SSC, 50 μ g/ml yeast tRNA, 50 μ g/ml heparin and 0.1% Tween 20) for 1 hour at 70°C and then hybridized with the specific probes overnight at 70°C in the same buffer. Unbound probes were removed by several post-hybridization washes (two washes of 30min in 50% formamide, 5xSSC at 70°C, followed by 2 washes of 30min each in Tris Buffer (0.1M Tris-HCl, 0.5M NaCl, 0.1% Tween 20) at RT and two washes of 30min in 50% formamide, 2xSSC at 70°C). After blocking for 1.5 hour at RT in blocking solution [10% normal goat serum (NGS), 2 mM levamisole] sections were incubated overnight at 4°C with alkaline phosphatase-conjugated antidigoxygenin antibodies (Roche; 1:2,000) diluted in TBST containing 1% NGS, 2 mM levamisole. After six washes of 30 min in TBST, sections were incubated for 2 \times 10 minutes in NTMT (100mM NaCl, 100mM Tris-HCl pH 9.5, 50mM MgCl₂, 0.1% Tween 20) and then in NBT/BCIP substrate (Roche) at RT to develop the signal. After overnight air-drying, slides were then coverslipped with DPX mounting media.

Generation of tamalin knockout mice

The ATG containing exon of the tamalin gene was targeted in mouse embryonic stem (ES) cells by a standard replacement-type targeting vector constructed by micro-homologous recombination in bacteria using a 129/SV mouse genomic fragment (Tessarollo et al., 2009). Electroporation and selection were performed using the CJ7 ES cell line as described elsewhere (Southon and Tessarollo, 2009). DNAs derived from G418/FIAU resistant ES clones were screened by a diagnostic BamHI restriction enzyme digestion using a 3 probe external to the targeting vector sequence. Recombinant clones containing the predicted rearranged band were obtained at a frequency of 1/4. Two independently targeted ES cell clones injected into C57BL/6 blastocysts generated chimeras that transmitted the mutated allele to the progeny (Reid and Tessarollo, 2009). Following germline transmission of the targeted ES cell clones, the diagnostic BamHI digest was used for screening as it enabled us to distinguish between the WT and all the targeted alleles including those generated after cre- or Flpe- recombination.

Mutant mice were backcrossed for at least 10 generations onto the C57BL/6 background before use. Animals of either sex were used for experimentation. Mice were bred in a specific, pathogen-free facility with food and water *ad libitum*. All experimental procedures followed the National Institutes of Health Guidelines for animal care and use, and were approved by the NCI-Frederick ACUC committee.

Behavioral Analysis

For a general behavioral characterization, mice were subjected to the elevated plus maze, as a measure of locomotor activity (number of crosses) and anxiety related behavior (time spent in an open arm) (Zhang et al., 2011); rota rod test (time spent on a rotating rod) to evaluate muscle strength and motor coordination (Wang et al., 2007); and forced swim test (immobility time) to detect possible depressive behavior phenotypes (Zhang et al., 2011).

BrdU injection Protocol

For basal cell proliferation studies, animals were injected with BrdU (200 mg/kg, i.p., Sigma) and sacrificed 2 hrs later. For basal cell survival studies, animals were injected with BrdU (200 mg/kg, i.p.) once daily for 3 consecutive days and sacrificed 28 days after the last BrdU injection (Yanpallewar et al., 2010). For analysis of ECS-induced proliferation of adult hippocampal progenitors WT and tamalin KO animals were subjected to ECS or sham treatment. Three days post-ECS, they were injected with BrdU (200 mg/kg i.p.) and perfused with 4% PFA 2 hrs later (Ma et al., 2009). For analysis of ECS-induced adult neurogenesis, animals were subjected to single ECS or sham treatment; 3 days later they were injected twice with BrdU (200mg/kg, i.p.) 12h apart, and sacrificed 28 days after the last BrdU injection (Madsen et al., 2000).

Immunohistochemistry and immunofluorescence

Brains perfused with 4% PFA were serially sectioned (50 μ m coronal cryostat sections), through the rostrocaudal extent of the hippocampus (Bregma -1.34 to -2.80 , Paxino and Franklin, The mouse brain in stereotaxic coordinates). One every fifth section was collected for BrdU, proliferating cell nuclear antigen (PCNA) or doublecortin (DCX) immunohistochemistry (6 sections/animal) as described previously (Yanpallewar et al., 2010). The primary antibodies were rat anti-BrdU antibody (1:500, Accurate Biochemicals), rabbit anti-PCNA (1: 250, SantaCruz) and goat anti-DCX antibody (1:500, SantaCruz). The secondary antibodies were biotinylated goat anti-rat or goat anti-rabbit (1:500 Vector Laboratories); biotinylated rabbit anti-goat (1:500, Vector Laboratories). Signal amplification was performed using a Vectastain Elite Avidin-Biotin (Vector Laboratories)

and visualization was done using diaminobenzidine (Sigma) as substrate. Quantification of the number of BrdU, PCNA and DCX-positive cells in tissue sections was carried out using an unbiased stereology protocol as described previously (Ma et al., 2009; Yanpallewar et al., 2010).

Double-labeled immunofluorescence staining was used to determine the co-localization of the BrdU signal with the mature neuronal marker NeuN (Madsen et al., 2000). Sections subjected to antigen retrieval were incubated with both rat anti-BrdU (1:500, Accurate Biochemicals) and mouse anti-NeuN (1:500 Millipore) antibodies overnight at RT. The secondary antibodies Alexa Fluor Goat anti-mouse 488 (1:500, Invitrogen) and Alexa Fluor goat anti-rat 568 (1:500 Invitrogen) were also used in combination for 2h. To address the effect of ECS on neurogenesis, the absolute number of BrdU+ cells that also express NeuN was determined by confocal microscopy. All BrdU+/NeuN+ cells (every 5th section, 6 sections in total per animal) were analyzed using z-plane confocal microscopy with 1 μ m steps (Zeiss LSM510 confocal microscope).

Timm Staining

Analysis of mossy fiber sprouting was done by using Timm staining as described previously (Vaidya et al., 1999). Animals received ECS or sham treatment for 10 consecutive days. Twelve days after the last treatment they were perfused with 0.37% sodium sulphide (Sigma) followed by 4% PFA. After overnight fixation in 4% PFA and cryoprotection with 30% sucrose, serial coronal sections (50 μ m) were cut on a cryostat through the rostrocaudal extent (Bregma -1.34 to -2.80, according to the Paxinos, G., Franklin, K.B.J., 2001. The mouse brain in stereotaxic coordinates. Academic Press, San Diego) of the hippocampus. One every fifth section (6 sections in total) was mounted on a slide, dried overnight and developed in the dark in a 12:6:2 mixture of Gum Arabic, hydroquinone and citrate buffer with 17% silver nitrate (Sigma). The intensity of Timm granules in the supragranular region of the hippocampal dentate gyrus (DG) was scored as follows (Vaidya et al., 1999): 0, no granules between the tip and the crest of the DG; 1, few granules with patchy distribution; 2, numerous granules with continuous distribution; 3, prominent granules in a continuous pattern with occasional patches of confluence; 4, prominent granules forming a laminar band; 5, a confluent dense laminar band of granules that extends into the inner molecular layer.

Golgi-Cox impregnation and Golgi tracing

Brains from animals sacrificed 12 days post-treatment were removed from the skull and immersed in Golgi-Cox solution (combination of Potassium Dichromate, HgCl₂ and Potassium Chromate pH 6.3–6.4, Sigma) in a glass bottle for 7 days at room temperature in the dark, then transferred to 30% sucrose until further processing. After at least 2 days in sucrose solution, coronal brain sections were serially cut at room temperature on a vibratome (125 μ m coronal sections) through the rostrocaudal extent of hippocampus (Bregma -1.46 to -3.40, according to Paxinos, G. and Franklin, K.B.J., 2001. The mouse brain in stereotaxic coordinates. Academic Press, San Diego). Sections from a single animal were collected in a well of a six well plate containing 30% sucrose, and mounted randomly (not sequentially) onto slides with 3% gelatin. Once on the slides, sections were brushed with 50% sucrose and allowed to air dry for 48 hours. They were then immersed in distilled water three times for 5 min with gentle shaking, transferred to a 4% KOH solution for 5–10 min, and again rinsed in distilled water. Following dehydration through graded ethanols, the slides were cleared with Histoclear (3 \times 5 min) and coverslipped with DPX mounting medium (Carim-Todd et al., 2009). To ensure random sampling, floating sections (12–14 per animal) were first collected in 30% sucrose and randomly mounted onto slides as described above. For tracing analysis, we started with the first section on the slide and

individual DG neurons that fulfilled the following selection criteria were included in the analysis. Neurons included in the analysis were chosen irrespective of rostrocaudal level or the number of the section on the slide. DG neurons selected for analysis of dendritic arborization of the primary dendrite had to fulfill the following criteria: 1, isolated cell body with a clear relationship of the primary dendrite to the soma; 2, presence of untruncated dendrites and dark impregnation along the extent of all of the dendrites; 3, relative isolation from neighboring impregnated cells that could interfere with the analysis. For each brain, 15 DG neurons were traced in 3D at 40X magnification using the NeuroLucida software (MicroBrightField, VT). The morphological traits of the cells (Dendritic branching and length) were measured in successive radial segments of 20 μm using the center of the soma as a reference point (Sholl Analysis). Sholl analysis was performed using Neuroexplorer (MicroBrightField) (Carim-Todd et al., 2009).

Western blot analysis

Brains were quickly removed, dissected and the resulting tissue samples were immediately frozen in dry ice. Following homogenization in NP40 lysis buffer, supernatants were collected, mixed with Laemmli Sample Buffer (2x, Sigma), boiled at 100°C for 5 min, and subjected to SDS-PAGE analysis. After separation by electrophoresis, proteins were transferred to PVDF membranes by electroblotting. Membranes were blocked in 5% milk in TBST, and incubated with a Rabbit anti-tamalin (1:1000, Rockland) or β -actin (1:1000, Santa Cruz) specific antibody overnight at 4°C. After washing, membranes were incubated with a donkey anti-rabbit HRP secondary antibody (1:2500, Millipore), washed again, and exposed to hyperfilm or to a Syngene Bioimaging System using the ECL detecting reagent (Amersham Biosciences). Band intensity quantification was done using either, Gene Snap Software (Syngene Bio-Imaging) or ImageQuant Software (Amersham Biosciences).

Electrophysiological recording

Electrophysiological recording was performed five hours after a single ECS. Three hours post-treatment, mice under isoflurane anaesthesia were decapitated and their brains were removed. Transverse hippocampal slices (350 μm thick) were obtained with a vibroslicer (Leica, Germany) in ice-cold Artificial Cerebro-Spinal Fluid (ACSF) containing (in mM): 125 NaCl, 1.25 KCl, 1 CaCl₂, 1.5 MgCl₂, 1.25 KH₂PO₄, 25 NaHCO₃, 16 glucose pH 7.4. Slices were incubated for 1 h at 32 °C in a surface chamber filled with ACSF in which CaCl₂ was raised to 2.5 mM, and a gas mixture (95% O₂, 5% CO₂) was continuously bubbled. After the first hour, temperature was reduced to 28 °C and slices were kept in the same chamber until the transfer to the recording chamber. Slices were perfused with ACSF at 28 °C at the rate of 2 mL/min. Field excitatory postsynaptic potentials (fEPSPs) were evoked in the molecular layer by stimulating the medial perforant path (MPP) in the DG with a teflon coated concentric platinum-iridium electrode and recorded with a borosilicate glass pipette pulled (Sutter P90) to obtain 4 MOhm tip resistance when filled with ACSF. An input/output curve was obtained by gradually increasing the stimulus intensity until the fEPSP reached a plateau. After that, the stimulus was reduced to obtain a fEPSP that was 50% of the maximum level. Baseline recording was obtained by stimulating the slice every 20 s for at least 45 minutes. Once the baseline was stabilized to obtain LTP, 3 \times 1 s, 100 Hz trains every 20 seconds were delivered to the stimulating electrode. Baseline recording was then resumed and followed for one hour. Field potential was recorded (Multiclamp 700b, Axon), digitized (10 KHz digidata 1324), low pass filtered (3 KHz, 8-pole Bessel) and stored (Clampex 9.2, Axon). Signals were analyzed off line (Clampfit 9.2, Axon) and the size of the fEPSP was evaluated by measuring the initial slope of the signal expressed as percentage of the variation from the baseline value (average of 5 minutes before the conditioning protocol). Results were further analyzed with IGOR pro 6.01 (WaveMetrics, U.S.A.). All data are reported as means \pm standard error.

Statistical Analysis

Data were analyzed using the Statistical Software GraphPad InStat and Prism (USA). Data from two groups were analyzed using unpaired Student's *t* test whereas results from more than two groups were subjected to statistical analysis by two-way (multivariate) ANOVA followed by post hoc Bonferroni test for group comparison. Two-way ANOVA was used to assess interaction between two factors, namely ECS treatment and genotype. For the Timm staining analysis we used a nonparametric statistical test- ANOVA followed by posthoc Dunn test- since the data are presented as scores. For Sholl analysis of dendritic length and intersections, we used repeated measures ANOVA followed by post hoc Bonferroni test for group comparison. A *P* value <0.05 was considered statistically significant.

Results

Tamalin is up-regulated in the dentate gyrus in response to Kainate and ECS

Since tamalin affects the adaptive neural plasticity involved in reinforcement of drug abuse (Ogawa et al., 2007) we decided to investigate whether it could influence adaptive neural plasticity events occurring in other paradigms.

We first characterized tamalin expression in response to neuronal excitation in the adult mouse hippocampus. We injected Kainate (10 mg/kg i.p.), an analogue of glutamic acid, since it has been shown to increase the activity of dentate granule cells in the hippocampus (Zagulska-Szymczak et al., 2001) (Fig. 1). In accordance with previous reports, we found hippocampal upregulation of the immediate early genes (IEGs) *arc* (activity related cytoskeletal protein), a classic activity-induced gene, (Fig. 1e–f) and *homer1a*, a scaffold protein that like tamalin has a PDZ-domain (Fig. 1c–d). Next, we evaluated whether tamalin expression was affected by kainate treatment. In situ hybridization analysis showed that tamalin is also up-regulated in the dentate gyrus (DG) of the hippocampus in response to kainate treatment, suggesting that tamalin mRNA levels are increased under conditions of enhanced excitatory neurotransmission (Fig. 1a–b). To investigate whether tamalin expression was affected in another paradigm of enhanced neurotransmission, we tested its expression following electroconvulsive shock (ECS), a treatment used in patients with major depression. As previously reported, animals given a single ECS show a significant up-regulation of *arc* in the DG [Fig. 1i–j; (Valentine et al., 2000)]. Interestingly, we found that hippocampal tamalin expression also increases after ECS, as compared to sham-treated animals (Fig. 1g–h). Again these data suggest that tamalin up-regulation may play a role in conditions of enhanced excitatory neurotransmission.

Next, to characterize the temporal changes of tamalin expression in response to ECS we subjected wild type mice to single ECS and evaluated tamalin mRNA levels at different time-points (Fig. 2). Specifically, the tamalin mRNA level begins to increase at 1h and peaks by 3h post-ECS before returning to control levels by 12h (Fig. 2a–f). Contrary to the transient increase produced by a single ECS, chronic ECS causes a longer lasting increase in tamalin that persisted at least up to 24h after the last ECS treatment (Fig. 2g, h). Interestingly, ECS causes not only an up-regulation in hippocampal tamalin mRNA but also in its protein level. In fact, chronic ECS leads to a robust 67% elevation in tamalin protein level ($p < 0.05$, Fig. 2i, left panels). Moreover, tamalin up-regulation is specific to the hippocampus since there is no significant change in the olfactory bulb or cortex, two other brain regions that also express tamalin (Fig. 2i, middle and right panels). Taken together, these data identify tamalin as a novel molecule showing dynamic changes in response to enhanced excitatory neurotransmission.

Tamalin is essential for the ECS-induced proliferation of hippocampal progenitors

Because of the clinical relevance of ECS for the treatment of chronic depression we decided to evaluate whether tamalin mediates events related to ECS-induced adult neuroplasticity. We focused on the DG of the hippocampus, one of the regions in the adult brain that retains the ability to generate new neurons in response to a variety of stimuli including ECS (Cameron and McKay, 2001; Madsen et al., 2000).

To this end, we generated a tamalin knockout (TKO) mouse model (Fig. 3). Tamalin deletion in the mouse does not cause any overt phenotype as also previously reported (Ogawa et al., 2007). Mutant mice are fertile, develop normally, have normal life span and are indistinguishable from WT controls [data not shown, (Ogawa et al., 2007)]. Anatomically, brains lacking tamalin do not show any gross morphological defects (data not shown). Moreover, in the elevated plus maze test, the forced swim test, and rota rod test no abnormalities were detected, suggesting normal sensory-motor and emotional behavior (Fig. 3d, e). Taken together, these data suggest that tamalin deficient mice do not have any overt developmental abnormalities. Next, we analyzed whether tamalin deficiency had an effect on adult hippocampal progenitor proliferation and survival. WT and TKO mice were injected with BrdU (200mg/kg i.p) and sacrificed 2h post BrdU for analysis of hippocampal progenitor proliferation. In agreement with a general lack of deficits in the mutant brains, we did not observe any effect in the basal proliferation and survival of adult hippocampal progenitors (Fig. 4a–d). Since ECS is known to increase hippocampal neurogenesis, we then assessed whether deletion of tamalin affects ECS-induced hippocampal progenitor proliferation (Madsen et al., 2000). Adult control and TKO mice were subjected to a single ECS and 3 days later were injected with BrdU (200mg/kg i.p), and sacrificed after 2 hours. Stereological analysis of BrdU+ cells showed a significant 88 % increase in proliferation in the hippocampus of WT animals while tamalin-mutant mice showed only a non-significant 10% increase as compared to sham-treated mice (Fig. 4e–i). Two-way ANOVA revealed a significant ECS and genotype interaction ($F_{(1, 14)} = 6.53, p < 0.05$). To further confirm the results obtained with the BrdU labeling, we performed an additional staining using the endogenous marker of cell division PCNA (proliferating cell nuclear antigen). Following single ECS, WT animals exhibited a 54% increase in PCNA+ cells while tamalin mutant mice showed only a mild, non-significant increase (Fig. 4j–n). Again, two-way ANOVA demonstrated a significant ECS \times genotype interaction ($F_{(1, 32)} = 5.87, p < 0.05$). Taken together, these data suggest that tamalin is critical for ECS-induced, but not basal, proliferation of adult hippocampal progenitors.

ECS-induced neurogenesis is blunted in tamalin knockout mice

DG analysis with BrdU and PCNA revealed that tamalin plays a critical role in regulating ECS-induced progenitor proliferation. To investigate whether ECS-induced hippocampal neurogenesis is also affected by tamalin deletion, we stained hippocampal sections from the groups used for the BrdU and PCNA analysis with doublecortin (DCX), a microtubule-associated phosphoprotein utilized as a marker of newly born neurons in the adult dentate gyrus (Rao and Shetty, 2004) (Fig. 5a–e). Stereological analysis showed a 30% increase in the number of DCX+ immature neurons in ECS-treated compared to sham-treated WT animals. However, tamalin-deficient mice failed to respond to the ECS-treatment since we did not detect any significant hippocampal increase in DCX+ cells when compared to sham-treated WT or TKO mice (Fig. 5a–e). Since this analysis provides information only on young, immature neurons, to further investigate whether tamalin affects the ECS-induced increase of mature neurons, we subjected the animals to single ECS, followed 3 days later by two BrdU injections (200mg/kg i.p.; 12 hours apart) to label a pool of proliferating progenitors. Twenty eight days post-BrdU injection, which allows enough time for the maturation and differentiation of BrdU labeled progenitors, the animals were sacrificed and

their hippocampal sections were double-stained for BrdU and the mature neuronal marker, NeuN. Analysis of double positive BrdU/NeuN cells, identified by the confocal z-plane sectioning method, showed that ECS-treated WT mice had about twice as many BrdU +NeuN+ cells when compared to sham-treated controls (Fig. 5f–i). Sham- or ECS-treated tamalin knockout mice had a similar number of BrdU+NeuN+ cells as sham-treated WT controls (Fig. 5f–i). Taken together, these data strongly suggests that tamalin is a critical mediator of ECS-induced neurogenesis.

Tamalin is required for ECS-induced mossy fiber sprouting and granule cells dendritic arborization

In addition to increasing adult neurogenesis, ECS also causes the sprouting of dentate granule cells that is believed to contribute to the ECS therapeutic effects (Sutula, 2002; Vaidya et al., 1999). Thus, we next assessed whether tamalin is involved in the regulation of hippocampal mossy fiber sprouting following chronic ECS. Animals were subjected to ECS for 10 consecutive days (one ECS daily) and sacrificed 12 days after the last treatment for mossy fiber sprouting analysis by Timm Staining. Consistent with a previous report (Vaidya et al., 1999), Timm staining of brains from WT control mice subjected to chronic ECS showed a robust increase in the intensity of Timm granules in the supragranular layer of the DG. However, in TKO mice this effect was blunted (Fig. 6a–e).

Seizure activity is known to cause an increase in the frequency of dentate granule cell basal dendrites (Ribak et al., 2000; Spigelman et al., 1998). Moreover, antidepressant treatments including ECS or fluoxetine administration have been shown to increase synaptogenesis, accelerate dendritic arborizations of newly generated neurons and spine maturation of DG cells (Chen et al., 2009; Wang et al., 2008; Zhao et al., 2011). However a direct demonstration of the effect of ECS on dendritic complexity of mature granule cells is still lacking. We therefore asked whether ECS can regulate the dendritic arborizations of mature granule cells and whether tamalin affects DG dendritic arborization in response to chronic ECS treatment. Animals were subjected to sham or chronic ECS, and DG neurons were visualized by Golgi-Cox staining, a direct method for the analysis of dendritic arborizations. Sholl analysis of neuron arborizations did not detect any difference in dendrite length or dendritic complexity between TKO or WT sham-treated animals under basal condition (Fig. 6f–j), again excluding developmental abnormalities in the mutant mice (Fig. 3). Following ECS, WT mice showed increased dendrite length and dendritic intersections at 60 μm and greater distances from the soma suggesting a robust response to the treatment (Fig. 6f–j). However, TKO mice did not respond to ECS since their DG neuron arborizations were indistinguishable from that of sham-treated mice. These results further suggest that while tamalin deletion does not affect basal neuronal morphology, it does affect neuronal sprouting after chronic ECS. Importantly, we made the novel observation that in addition to enhancing hippocampal neurogenesis, ECS also stimulates apical dendritic arborization of DG cells, a function blunted by tamalin deletion.

Tamalin affects LTP response after ECS

Tamalin is a multimodular scaffold protein that forms a protein complex with 1/2 metabotropic glutamate receptors, guanine nucleotide exchange factor cytohesins as well as other scaffold proteins such as PSD-95, Mint2 and CASK which are involved in postsynaptic organization and protein trafficking (Kitano et al., 2003). Therefore, we asked whether loss of tamalin may affect synaptic transmission in basal conditions or after ECS. We found that LTP, at 1h in granule cells of the DG, induced by high frequency stimulation of the medial perforant path was similar between WT and TKO mice, suggesting that loss of tamalin does not affect this aspect of hippocampal synaptic plasticity (Fig. 7). Furthermore, the basal synaptic transmission appeared to be normal, as assessed by the input–output

curves (stimulus intensity vs fEPSP slope; data not shown). However, following ECS, 1 h LTP was almost completely abolished in TKO mice while in WT animals it was only slightly reduced compared to animals that did not undergo ECS (not statistically significant; Fig. 7a). The input/output curve was also altered in the TKO compared to the WT mice since in the TKO it reached the maximal fEPSP amplitude earlier than in the WT (Fig. 7c). The nature of this difference is unclear and needs to be further investigated.

Discussion

In this study we have identified tamalin as a scaffold protein that is both up-regulated by ECS and required for the increased hippocampal neurogenesis and DG neuron arborizations in response to ECS. These findings establish tamalin as one of the key mediator of ECS-induced adult neuroplasticity. ECS is the most effective therapy for patients with severe depression. However, the availability of pharmacological antidepressants and the need to induce electroconvulsion in patients for ECS therapy to provide therapeutic benefit, has made it an unpopular treatment choice restricting its use to treating drug-resistant or suicidal patients (Kato, 2009). This suggests that the identification of genes that are critical in the mediation of ECS effects may help dissect out the pathways that produce the positive effects of this treatment against depression without the need to induce electroconvulsion. Microarray studies have identified at least 120 genes, including transcription factors, neurotrophins, neurotransmitters and neuropeptides that show an altered pattern of expression after ECS (Altar et al., 2004; Newton et al., 2003). Moreover, analysis of the activity regulated transcription factor cAMP response element binding protein (CREB) has shown increased occupancy of at least 27 promoters in the hippocampus following ECS (Tanis et al., 2008). Thus, while it has been challenging to establish which of these genes are required to translate specific neurochemical changes into cellular and structural alterations, it is somewhat surprising that a single gene like tamalin, that does not have obvious developmental roles, is necessary to mediate two major ECS effects (Kato, 2009). Scaffolding proteins, by means of their protein-protein interaction domains, provide a platform for regulating multiple pathways linking intracellular and extracellular events to orchestrate neuronal signaling and function. The scaffold protein tamalin interacts with group 1 and 2 metabotropic glutamate receptors, specific guanine nucleotide exchange factors, postsynaptic and protein-trafficking scaffold proteins such as PSD95, Mint2 and CASK, as well as signaling molecules like neurotrophin receptors and src and syk kinases (Esteban et al., 2006; Hirose et al., 2004; Kitano et al., 2003). Thus, through these complex interactions tamalin appears to control a variety of pathways that are involved in the mediation of ECS effects. For example, neuronal progenitor proliferation may be stimulated by activating the src and syk tyrosine kinases that are expressed in the hippocampus and whose downstream signaling effectors include phospholipase C-gamma, protein kinase C, PI3-kinase, ras, MAPK and CREB (Hatterer et al., 2011; Hirose et al., 2004; Sada et al., 2001; Tian et al., 2009). Moreover, by activating the cytohesin-2-Rac1 pathway and its effectors PAKs (p21-activated kinases) tamalin may contribute to the cytoskeletal rearrangements that are essential for promoting neurite outgrowth (Bokoch, 2003; Esteban et al., 2006; Rex et al., 2007). One question that is still unresolved is how can tamalin exert these biological effects? Recently, Sugi and colleagues (2007), based on crystal structure and biochemical data have proposed a model by which tamalin, at low concentrations self-assembles into a weak-dimeric autoinhibited conformation through its PDZ domain and the C-terminal intrinsic ligand motif (Sugi et al., 2007). However, when its concentration increases tamalin forms tetramers that in the presence of dimeric mGluR stabilize the PDZ-mediated dimerization and contribute to amplifying the assembly of signaling molecules (Sugi et al., 2007). This model appears in agreement with our findings since we have shown that ECS induces tamalin up-regulation. In turn, an increase in tamalin concentration would cause the assembly of signaling molecules that are required to promote neurogenesis and

neuronal sprouting in response to ECS. In this scenario tamalin deletion is not expected to affect the expression of molecules such as mGluR5, which is indeed what we have observed in preliminary analysis (data not shown). This model would also explain why tamalin deletion does not have obvious developmental effects but can instead have such a profound effect on specific neuroplasticity-associated events. In fact, tamalin at basal, low levels would be present mainly in the inactive form and its removal would have no major impact on development. In contrast, genes such as BDNF and VEGF, that are also required for ECS-mediated neuroplasticity, activate receptors and signaling pathways that are critical for normal developmental (Segi-Nishida et al., 2008; Vaidya et al., 1999). Therefore, while BDNF or VEGF are upstream regulators of neurogenesis and neuronal plasticity, tamalin appears to be up-regulated only in response to unique situations of enhanced excitatory neurotransmission. Thus, it promotes the assembling/recruitment of the signaling pathways components that mediate only specific adult neuroplasticity-related events (Ogawa et al., 2007). In the future it will be important to establish which tamalin-regulated pathways are contributing to the individual changes caused by ECS. Taken together, our data strongly suggest that tamalin is an important mediator of ECS-induced neurogenesis and neuronal sprouting in the adult brain. Understanding which specific pathways are activated by tamalin may help provide critical targets to develop drugs that mediate the beneficial effects of ECS to treat severe depression.

Acknowledgments

We thank Eileen Southon and Susan Reid for technical help in generating the tamalin mutant mouse model, Jodi Becker for technical help and Dr. Mehdi Tufti for the homer1a construct. This research was supported by the Intramural Research Program of the NCI, Center for Cancer Research, NIH.

References

- Altar CA, Laeng P, Jurata LW, Brockman JA, Lemire A, Bullard J, Bukhman YV, Young TA, Charles V, Palfreyman MG. Electroconvulsive seizures regulate gene expression of distinct neurotrophic signaling pathways. *The Journal of Neuroscience*. 2004; 24:2667–2677. [PubMed: 15028759]
- Bokoch GM. Biology of the p21-activated kinases. *Annu Rev Biochem*. 2003; 72:743–781. [PubMed: 12676796]
- Cameron HA, McKay RD. Adult neurogenesis produces a large pool of new granule cells in the dentate gyrus. *J Comp Neurol*. 2001; 435:406–417. [PubMed: 11406822]
- Carim-Todd L, Bath KG, Fulgenzi G, Yanpallewar S, Jing D, Barrick CA, Becker J, Buckley H, Dorsey SG, Lee FS, Tessarollo L. Endogenous truncated TrkB.T1 receptor regulates neuronal complexity and TrkB kinase receptor function in vivo. *J Neurosci*. 2009; 29:678–685. [PubMed: 19158294]
- Chen F, Madsen TM, Wegener G, Nyengaard JR. Repeated electroconvulsive seizures increase the total number of synapses in adult male rat hippocampus. *Eur Neuropsychopharmacol*. 2009; 19:329–338. [PubMed: 19176277]
- Esteban PF, Yoon HY, Becker J, Dorsey SG, Caprari P, Palko ME, Coppola V, Saragovi HU, Randazzo PA, Tessarollo L. A kinase-deficient TrkC receptor isoform activates Arf6-Rac1 signaling through the scaffold protein tamalin. *J Cell Biol*. 2006; 173:291–299. [PubMed: 16636148]
- Fagni L, Worley PF, Ango F. Homer as both a scaffold and transduction molecule. *Sci STKE*. 2002; 2002:re8. [PubMed: 12072556]
- Hatterer E, Benon A, Chounlamountri N, Watrin C, Angibaud J, Jouanneau E, Boudin H, Honnorat J, Pellier-Monnin V, Noraz N. Syk kinase is phosphorylated in specific areas of the developing nervous system. *Neurosci Res*. 2011; 70:172–182. [PubMed: 21354221]
- Hirose M, Kitano J, Nakajima Y, Moriyoshi K, Yanagi S, Yamamura H, Muto T, Jingami H, Nakanishi S. Phosphorylation and recruitment of Syk by immunoreceptor tyrosine-based activation

- motif-based phosphorylation of tamalin. *J Biol Chem.* 2004; 279:32308–32315. [PubMed: 15173175]
- Jiang X, Tian F, Du Y, Copeland NG, Jenkins NA, Tessarollo L, Wu X, Pan H, Hu XZ, Xu K, Kenney H, Egan SE, Turley H, Harris AL, Marini AM, Lipsky RH. BHLHB2 controls Bdnf promoter 4 activity and neuronal excitability. *J Neurosci.* 2008; 28:1118–1130. [PubMed: 18234890]
- Kato N. Neurophysiological mechanisms of electroconvulsive therapy for depression. *Neurosci Res.* 2009; 64:3–11. [PubMed: 19321135]
- Kitano J, Yamazaki Y, Kimura K, Masukado T, Nakajima Y, Nakanishi S. Tamalin is a scaffold protein that interacts with multiple neuronal proteins in distinct modes of protein-protein association. *J Biol Chem.* 2003; 278:14762–14768. [PubMed: 12586822]
- Ma DK, Jang MH, Guo JU, Kitabatake Y, Chang ML, Pow-Anpongkul N, Flavell RA, Lu B, Ming GL, Song H. Neuronal activity-induced Gadd45b promotes epigenetic DNA demethylation and adult neurogenesis. *Science.* 2009; 323:1074–1077. [PubMed: 19119186]
- Madsen TM, Treschow A, Bengzon J, Bolwig TG, Lindvall O, Tingstrom A. Increased neurogenesis in a model of electroconvulsive therapy. *Biol Psychiatry.* 2000; 47:1043–1049. [PubMed: 10862803]
- Malberg JE, Eisch AJ, Nestler EJ, Duman RS. Chronic antidepressant treatment increases neurogenesis in adult rat hippocampus. *J Neurosci.* 2000; 20:9104–9110. [PubMed: 11124987]
- Newton SS, Collier EF, Hunsberger J, Adams D, Terwilliger R, Selvanayagam E, Duman RS. Gene profile of electroconvulsive seizures: induction of neurotrophic and angiogenic factors. *J Neurosci.* 2003; 23:10841–10851. [PubMed: 14645477]
- Ogawa M, Miyakawa T, Nakamura K, Kitano J, Furushima K, Kiyonari H, Nakayama R, Nakao K, Moriyoshi K, Nakanishi S. Altered sensitivities to morphine and cocaine in scaffold protein tamalin knockout mice. *Proc Natl Acad Sci U S A.* 2007; 104:14789–14794. [PubMed: 17766434]
- Rao MS, Shetty AK. Efficacy of doublecortin as a marker to analyse the absolute number and dendritic growth of newly generated neurons in the adult dentate gyrus. *Eur J Neurosci.* 2004; 19:234–246. [PubMed: 14725617]
- Reid SW, Tessarollo L. Isolation, microinjection and transfer of mouse blastocysts. *Methods Mol Biol.* 2009; 530:269–285. [PubMed: 19266343]
- Rex CS, Lin CY, Kramar EA, Chen LY, Gall CM, Lynch G. Brain-derived neurotrophic factor promotes long-term potentiation-related cytoskeletal changes in adult hippocampus. *J Neurosci.* 2007; 27:3017–3029. [PubMed: 17360925]
- Ribak CE, Tran PH, Spigelman I, Okazaki MM, Nadler JV. Status epilepticus-induced hilar basal dendrites on rodent granule cells contribute to recurrent excitatory circuitry. *J Comp Neurol.* 2000; 428:240–253. [PubMed: 11064364]
- Sada K, Takano T, Yanagi S, Yamamura H. Structure and function of Syk protein-tyrosine kinase. *J Biochem.* 2001; 130:177–186. [PubMed: 11481033]
- Sakagami Y, Yamamoto K, Sugiura S, Inokuchi K, Hayashi T, Kato N. Essential roles of Homer-1a in homeostatic regulation of pyramidal cell excitability: a possible link to clinical benefits of electroconvulsive shock. *Eur J Neurosci.* 2005; 21:3229–3239. [PubMed: 16026461]
- Segi-Nishida E, Warner-Schmidt JL, Duman RS. Electroconvulsive seizure and VEGF increase the proliferation of neural stem-like cells in rat hippocampus. *Proc Natl Acad Sci U S A.* 2008; 105:11352–11357. [PubMed: 18682560]
- Southon E, Tessarollo L. Manipulating mouse embryonic stem cells. *Methods Mol Biol.* 2009; 530:165–185. [PubMed: 19266324]
- Spigelman I, Yan XX, Obenaus A, Lee EY, Wasterlain CG, Ribak CE. Dentate granule cells form novel basal dendrites in a rat model of temporal lobe epilepsy. *Neuroscience.* 1998; 86:109–120. [PubMed: 9692747]
- Sugi T, Oyama T, Muto T, Nakanishi S, Morikawa K, Jingami H. Crystal structures of autoinhibitory PDZ domain of Tamalin: implications for metabotropic glutamate receptor trafficking regulation. *Embo J.* 2007; 26:2192–2205. [PubMed: 17396155]
- Sutula T. Seizure-Induced Axonal Sprouting: Assessing Connections Between Injury, Local Circuits, and Epileptogenesis. *Epilepsy Curr.* 2002; 2:86–91. [PubMed: 15309153]

- Tanis KQ, Duman RS, Newton SS. CREB binding and activity in brain: regional specificity and induction by electroconvulsive seizure. *Biol Psychiatry*. 2008; 63:710–720. [PubMed: 17936724]
- Tessarollo L, Palko ME, Akagi K, Coppola V. Gene targeting in mouse embryonic stem cells. *Methods Mol Biol*. 2009; 530:141–164. [PubMed: 19266325]
- Tian HP, Huang BS, Zhao J, Hu XH, Guo J, Li LX. Non-receptor tyrosine kinase Src is required for ischemia-stimulated neuronal cell proliferation via Raf/ERK/CREB activation in the dentate gyrus. *BMC Neurosci*. 2009; 10:139. [PubMed: 19943942]
- Vaidya VA, Siuciak JA, Du F, Duman RS. Hippocampal mossy fiber sprouting induced by chronic electroconvulsive seizures. *Neuroscience*. 1999; 89:157–166. [PubMed: 10051225]
- Valentine G, Chakravarty S, Sarvey J, Bramham C, Herkenham M. Fragile X (fmr1) mRNA expression is differentially regulated in two adult models of activity-dependent gene expression. *Brain Res Mol Brain Res*. 2000; 75:337–341. [PubMed: 10686356]
- Wang JW, David DJ, Monckton JE, Battaglia F, Hen R. Chronic fluoxetine stimulates maturation and synaptic plasticity of adult-born hippocampal granule cells. *J Neurosci*. 2008; 28:1374–1384. [PubMed: 18256257]
- Wang Y, Mao XO, Xie L, Banwait S, Marti HH, Greenberg DA, Jin K. Vascular endothelial growth factor overexpression delays neurodegeneration and prolongs survival in amyotrophic lateral sclerosis mice. *J Neurosci*. 2007; 27:304–307. [PubMed: 17215390]
- Yanpallewar SU, Fernandes K, Marathe SV, Vadodaria KC, Jhaveri D, Rommelfanger K, Ladiwala U, Jha S, Muthig V, Hein L, Bartlett P, Weinshenker D, Vaidya VA. Alpha2-adrenoceptor blockade accelerates the neurogenic, neurotrophic, and behavioral effects of chronic antidepressant treatment. *J Neurosci*. 2010; 30:1096–1109. [PubMed: 20089918]
- Zagulska-Szymczak S, Filipkowski RK, Kaczmarek L. Kainate-induced genes in the hippocampus: lessons from expression patterns. *Neurochem Int*. 2001; 38:485–501. [PubMed: 11248397]
- Zhang LL, Wang JJ, Liu Y, Lu XB, Kuang Y, Wan YH, Chen Y, Yan HM, Fei J, Wang ZG. GPR26-deficient mice display increased anxiety- and depression-like behaviors accompanied by reduced phosphorylated cyclic AMP responsive element-binding protein level in central amygdala. *Neuroscience*. 2011; 196:203–214. [PubMed: 21924326]
- Zhao C, Warner-Schmidt J, Duman R, Gage FH. Electroconvulsive seizure promotes spine maturation in newborn dentate granule cells in adult rat. *Dev Neurobiol*. 2011

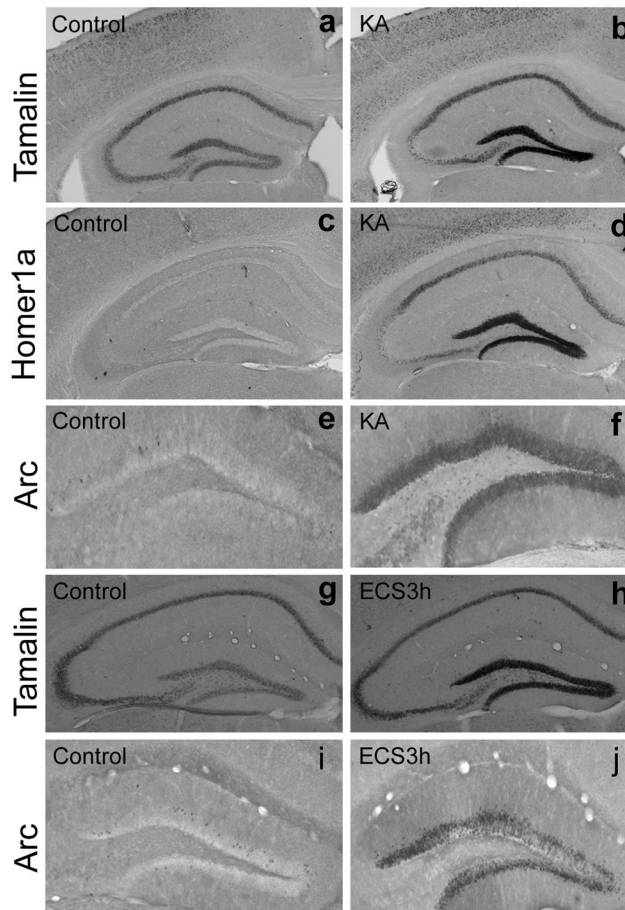


Figure 1. Tamalin mRNA expression is up-regulated in the dentate gyrus of adult mice after kainate administration and ECS

Representative in situ hybridization (a–d; g, h) and immunohistochemistry (e, f, i, j) analysis performed respectively with tamalin (a, b g, h) or homer1a (c, d) specific probes and an arc-specific antibody (e, f, i, j). Adult animals were injected with vehicle (a, c, e) or kainate (10 mg/kg i.p.; b, d, f) and sacrificed 3 hr later for in situ hybridization or immunohistochemistry analysis. Homer1a and arc, established immediate early genes, were used as positive controls. Note tamalin mRNA expression is up-regulated in response to kainate (b) similarly to homer1a mRNA (d) and arc protein (f). ECS also causes an increase in Arc immunoreactivity (j) and tamalin mRNA (h) 3 hours after treatment in the dentate gyrus of the hippocampus when compared to control animals (i and g respectively). n=4 animals for each analysis.

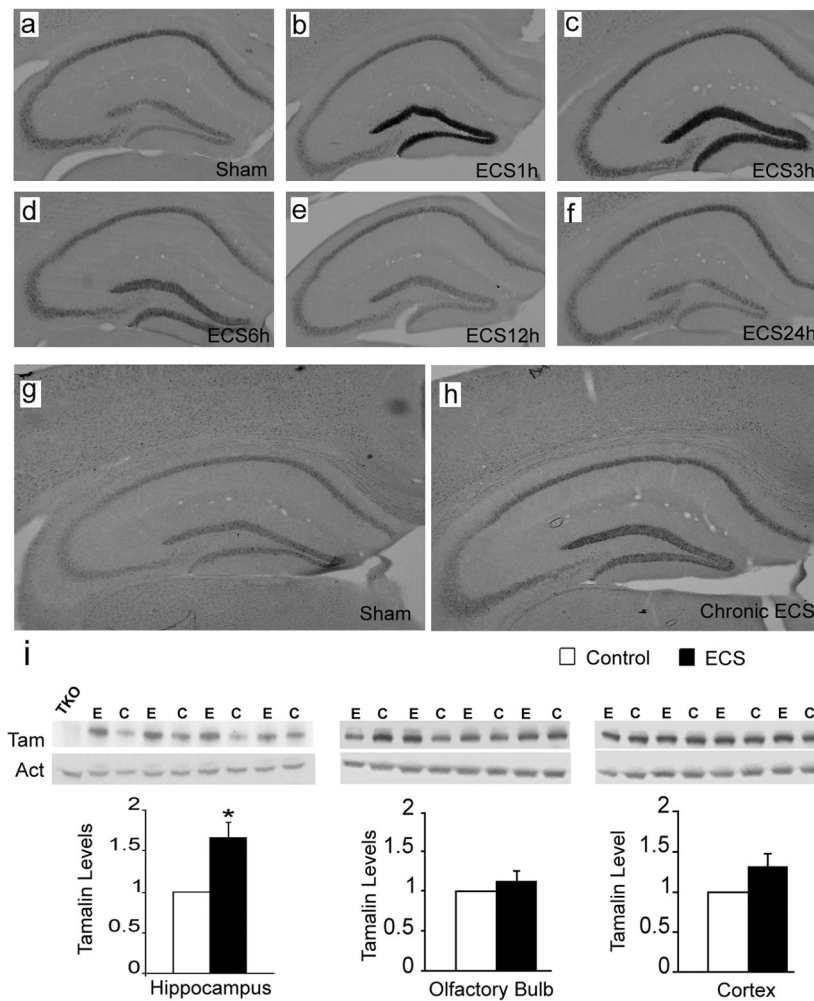


Figure 2. Hippocampal tamalin mRNA and protein are up-regulated in response to ECS

Representative tamalin in situ hybridization analysis of hippocampus from mice after single (a–f) or chronic (g, h) ECS. Sham-treated animals show the basal level of tamalin expression (a, g). Tamalin mRNA is up regulated at 1 hour (b) and peaks at 3 hours (c) from ECS. Beginning at 6 hours (d) tamalin is down regulated and returns to the pre-ECS level by 12 (e) and 24 hours (f). Note that tamalin mRNA expression remains up-regulated at 24 hours after chronic ECS (h) as compared to sham-treated controls (g). $n=4$ for each group. Expression of tamalin protein after chronic ECS (i). Animals received one ECS a day for 5 consecutive days and were sacrificed 24 hrs after the last treatment. Western blot analysis of hippocampus (left panel), olfactory bulb (central panel) and cortex (right panel) from ECS (E)- or sham (C)-treated WT animals using an anti-tamalin antibody (Tam); b-actin was used as loading control (Act) and a hippocampus lysate from a tamalin KO mouse was used as negative control (TKO). The quantification of tamalin protein levels is shown at the bottom. Note the selective tamalin up regulation in the hippocampus. $n = 4$ animal. $P < 0.05$ students 't' test.

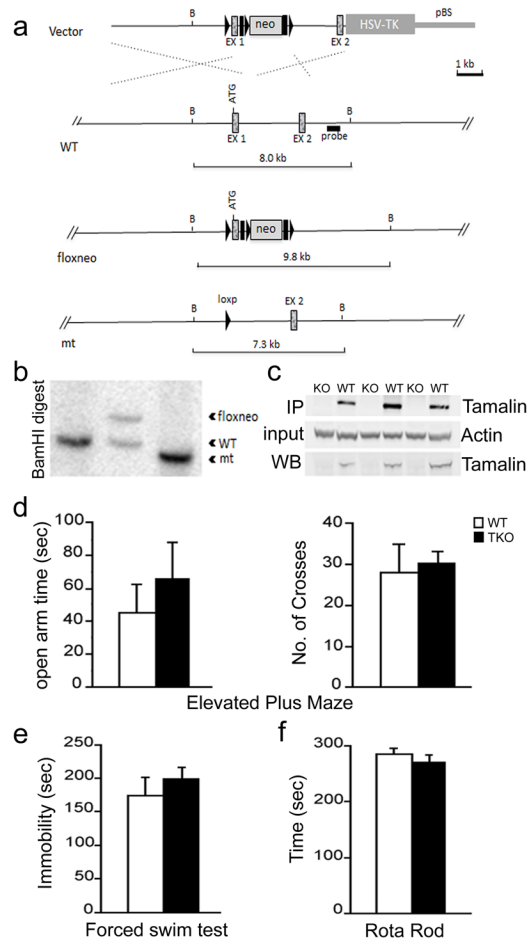


Figure 3. Targeted deletion of tamalin in mouse

Schematic representation of the strategy used to target the *tamalin* gene. LoxP sites (black triangles) were inserted upstream and downstream of the ATG containing exon 1 (EX1). The neomycin resistance cassette (neo) is flanked by both loxP and Frt (black rectangles) sites. After the initial screening of the positive ES cell clones, as described in Material and Methods, a probe (black rectangle) downstream of EX1 was used for the identification of the different targeted alleles by detecting a shift from the endogenous *Bam*HI wild-type (WT) band of 8 kb to the rearranged 9.8 Kb band resulting from the insertion of the neo cassette by homologous recombination. Cre-induced excise of the tamalin-specific exon and the neo cassette causes a shift of the 9.8 Kb band to 7.3 Kb. (b) Southern analysis of genomic DNA from mice with the tamalin alleles indicated in (a). Analysis of DNA digested with the BamHI restriction enzyme and probed with the 3' fragment described in (a) yields the expected 8 Kb band in a WT mouse (lanes 1) and a rearranged 9.8 Kb fragment with the neo insertion (floxneo) in a heterozygous mouse and a 7.3 Kb band in the mutant (lane 2 and 3 respectively). (c) Western blot analysis of hippocampus dissected from mutant (KO) or WT mice and hybridized with an antiserum directed against tamalin. The top panel is a western analysis of lysates subjected first to I.P with a tamalin specific antibody and then to the blotting with the same antibody. The bottom panel is the western analysis of straight hippocampus lysates hybridized with the tamalin-specific antibody. The middle blot was hybridized with an anti-B-actin-specific antibody to control for loading. Behavioral analysis of tamalin-deficient mice (d–f). Animals were subjected to the elevated plus maze (d), forced swim (e) and rota-rod (f) test. n = 7.

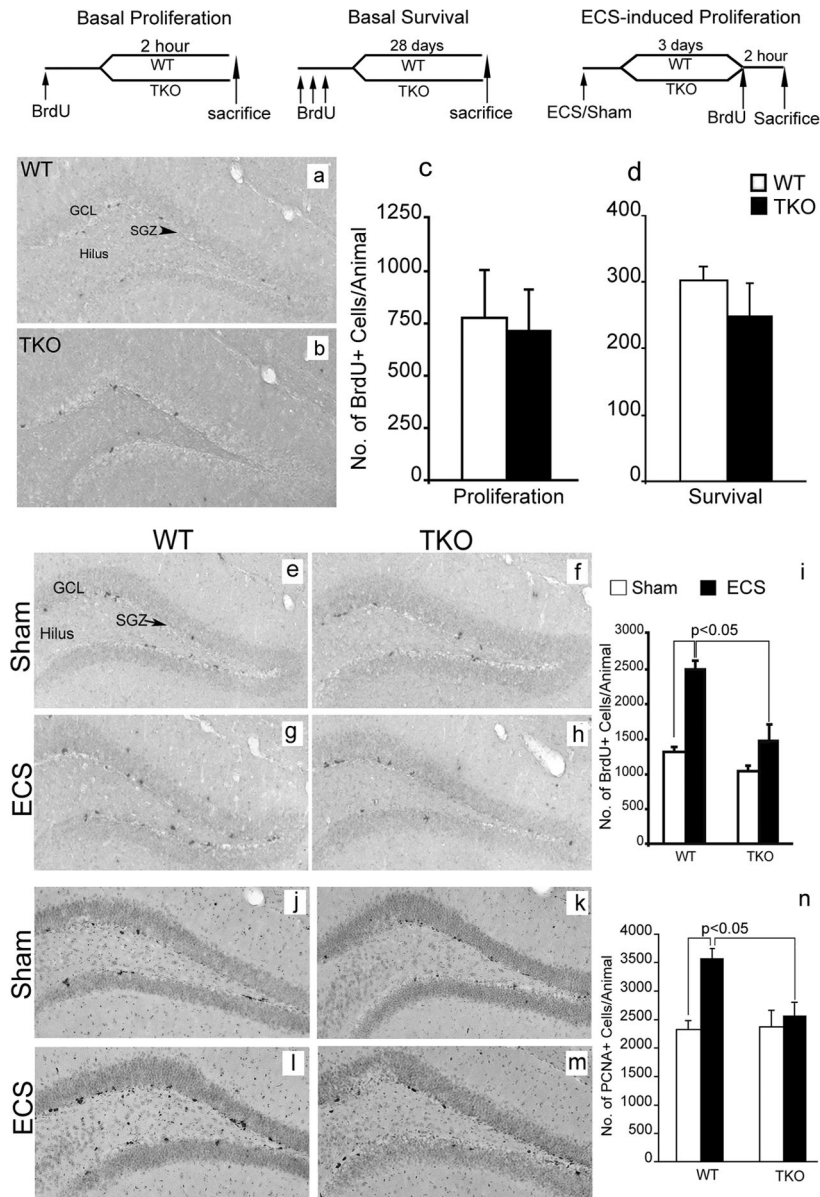


Figure 4. Tamalin deficiency blocks ECS-induced proliferation of adult hippocampal progenitors

BrdU staining of representative hippocampal sections from WT (a) and tamalin KO (b) mice showing BrdU+ hippocampal progenitors in the subgranula zone (SGZ, arrowhead) of the DG, 2h post BrdU injection. (c, d): Quantification of BrdU+ cells in the SGZ of the hippocampus showing no changes in basal progenitors proliferation (c) or survival (d) in WT and Tamalin KO mice. The data analyzed by student's t test represent the mean \pm SEM; n = 4–5 per group. (e–h): Representative BrdU immunohistochemistry images from sham (e, f) or ECS-treated (g, h) WT (e, g) and tamalin KO (f, h) animals. Note the mild, non significant, increase of ECS-induced BrdU+ proliferating progenitors in the SGZ of the DG of TKO mice compared to the robust increased in the WT animals (i). (j–m) Representative photomicrographs of PCNA+ cells as in (e–h). Note the significant increase in the number of PCNA+ cells only in the ECS-treated WT animals (n). Data in (i, n) was analyzed by two-way ANOVA followed by *post hoc* Bonferroni test and represent the Mean \pm SEM. n = 8–

10 per group. Two-way ANOVA revealed a significant ECS and genotype interaction for data presented in (i) ($F_{(1, 14)} = 6.53, p < 0.05$) and (n) ($F_{(1, 32)} = 5.87, p < 0.05$). The schedules of BrdU injection and analysis for the basal proliferation (c), survival (d) and ECS-induced proliferation (i, n) are depicted at the top. GCL, granular cell layer.

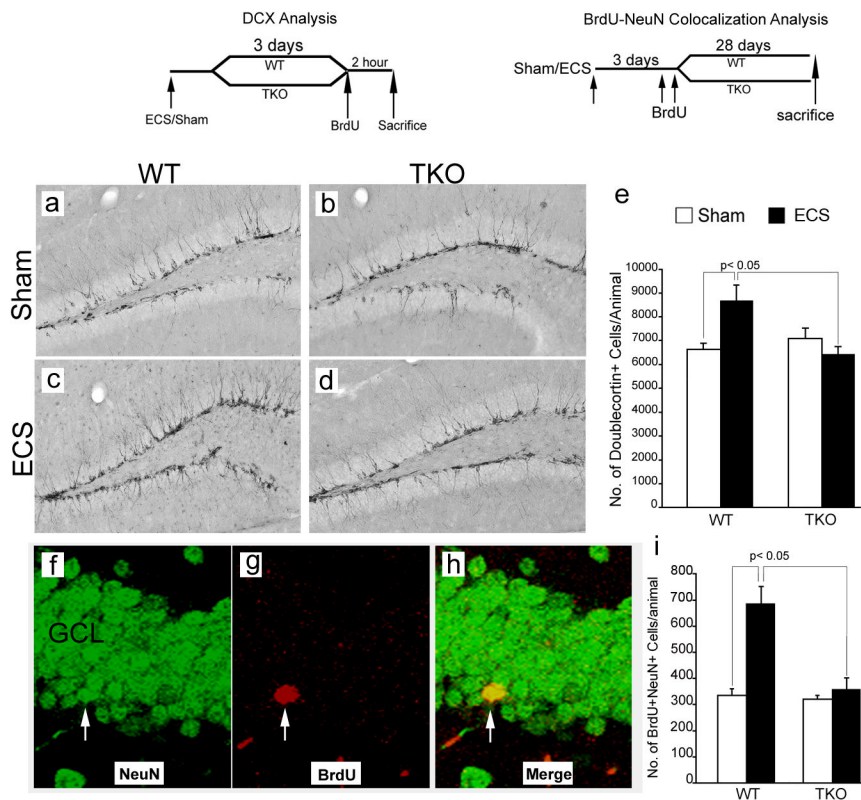


Figure 5. Tamalin is required for ECS-induced hippocampal neurogenesis
 (a–d): Representative immunohistochemistry images showing doublecortin-positive (DCX+; a marker for immature neurons) cells in the dentate gyrus of WT (a, c) and Tamalin KO (b, d) animals subjected to sham (a, b) or ECS treatment (c, d). (e): Quantitative analysis of DCX+ cells showing an increase in the number of immature neurons caused by ECS in WT but not in tamalin KO animals. n = 6–8 animals per group. (f–h): Confocal z-stack representative images showing co-localization of BrdU+ cells with NeuN, a marker for mature neurons. WT and Tamalin KO animals were subjected to a single sham or ECS treatment and they were injected with BrdU (200mg/kg i.p.) three days later. (i): Quantitative analysis showing the increase in the number of BrdU/NeuN double positive cells caused by ECS in WT animals but not in tamalin KO mice. n = 4–7 animals per group. Data represent the Mean ± SEM analyzed by two way ANOVA followed by Bonferroni posthoc test. Two-way ANOVA demonstrated a significant ECS-genotype interaction in both the DCX (e) ($F_{(1, 24)} = 8.01, p < 0.05$) and NeuN/BrdU (i) ($F_{(1, 19)} = 8.77, p < 0.05$) analysis. The schedules of BrdU injection and DCX or BrdU/NeuN analysis are depicted at the top.

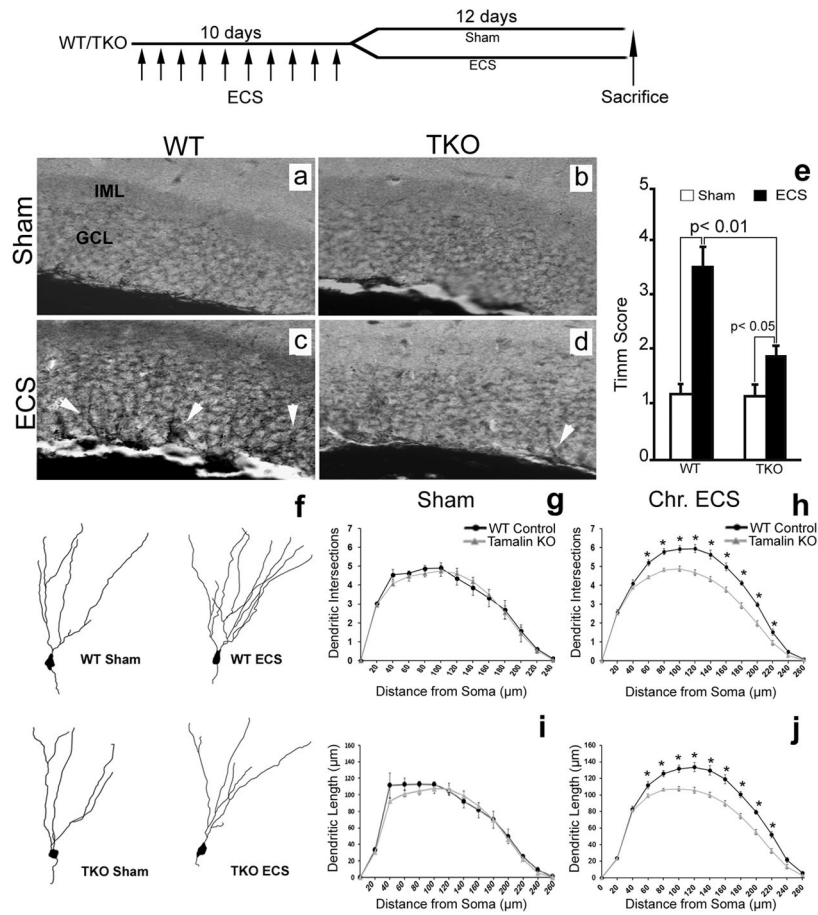


Figure 6. Chronic ECS-induced neuronal sprouting is blunted in tamalin KO mice
 Analysis of mossy fiber sprouting by Timm staining (a–e) and dendritic complexity of dentate granule cells by Golgi-cox staining (f–j). Representative Timm-stained hippocampal sections from sham (a, b) or chronic ECS-treated (c, d) WT (a, c) or TKO (b, d) mice. Note the reduced presence of Timm granules (white arrowheads in c,d) in the GCL of the hippocampus of ECS-treated TKO mice compared to ECS-treated control mice (n = 5 animals for each group). (e) Quantitative analysis of Timm scores. Data representing the Mean \pm SEM was analyzed by nonparametric ANOVA followed by posthoc Dunn test. (f) Representative neuroLucida reconstruction of DG Golgi-stained neurons from sham- or chronic ECS-treated WT and TKO mice. (g–j) Sholl analysis of dendritic intersection number and dendrite length of DG neurons showing no difference between sham-treated WT and tamalin KO mice (g–i; n=5 mice in each group; 15 neurons/mouse). Only EC-treated WT animals display a significant increase in the number of intersections (h) and dendritic length (j) compared to sham treated controls (n = 9 mice in each group; 15 neurons/mouse). * $p < 0.05$. Data represent the Mean \pm SEM analyzed by two way ANOVA followed by Bonferroni posthoc test. Top: schematic indicating that Sham or Chronic ECS-treated (once a day for 10 consecutive days) animals were sacrificed 12 days after the last ECS.

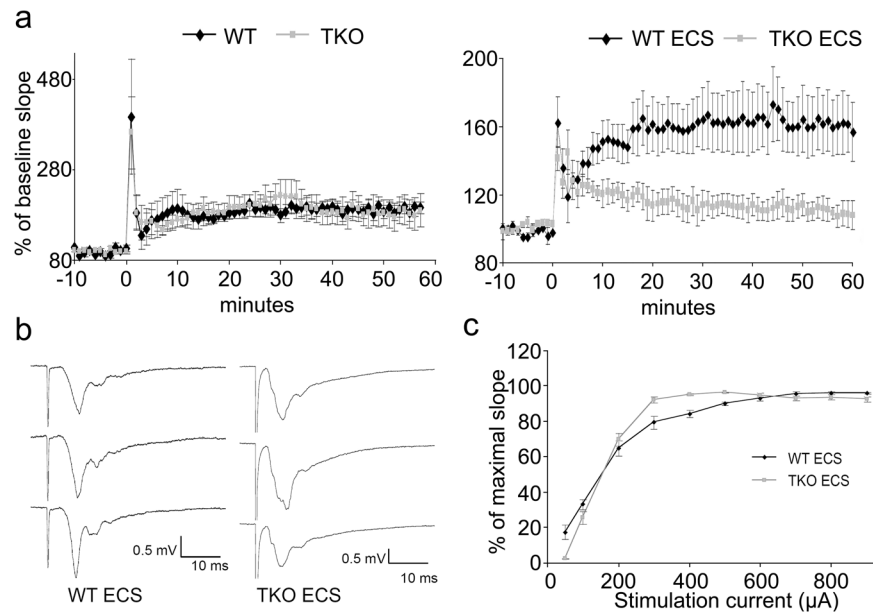


Figure 7. Tamalin deficiency blocks LTP formation after ECS

Three 100 Hz, 1 second-long stimuli train, induced an immediate post-tetanic potentiation (PTP) lasting few minutes then a long term potentiation lasting several hours (LTP). (a): Time course of Field excitatory postsynaptic potentials (fEPSPs) evoked in the molecular layer of the DG by stimulating the medial perforant path. Slope at baseline (–10 to 0 min) and after induction of LTP (0 time mark). Points are average of traces from 4 WT and 4 TKO with and without ECS. Without ECS no differences are evident in TKO with respect to WT mice. ECS blunted the LTP formation in TKO but did not alter PTP. Note that ECS administered 5 hours before LTP recording blunted the response in WT but the reduction in LTP was much more pronounced in the TKO mice. (b): fEPSP recorded in DG. Traces from top to bottom identify baseline fEPSP before LTP induction, 1 minute after induction and 1 h after induction. (c): Input–Output curve obtained before LTP induction in TKO and WT mice that underwent ECS.